Annals of Biomedical Engineering, Vol. 51, No. 1, January 2023 *(© 2022)* pp. 24–33
https://doi.org/10.1007/s10439-022-03018-8

S.I. : Modeling for Advancing Regulatory Science

A Validated Open-Source Shoulder Finite Element Model and Investigation of the Effect of Analysis Precision

Sara Sadeqi,[1,2] Andrew P. Baumann,[2] Vijay K. Goel,[1] Victoria Lilling,[3] and Stacey J. L. Sullivan[2]

[1]Departments of Bioengineering and Orthopaedics, Engineering Center for Orthopaedic Research Excellence (E-CORE), The University of Toledo, Toledo, OH, USA; [2]Center for Devices and Radiological Health, Office of Science and Engineering Laboratories, Division of Applied Mechanics, U.S. Food and Drug Administration, 10903 New Hampshire Avenue, Building 62 Room 2210, Silver Spring, MD 20993, USA; and [3]Center for Devices and Radiological Health, Office of Product Evaluation and Quality, OHT6: Office of Orthopedic Devices, DHT6A: Division of Joint Arthroplasty Devices, Shoulder Arthroplasty Devices Team, U.S. Food and Drug Administration, Silver Spring, MD, USA

(Received 15 April 2022; accepted 7 July 2022; published online 26 July 2022)

Associate Editor Joel Stitzel oversaw the review of this article.

Abstract—Understanding the loads and stresses on different tissues within the shoulder complex is crucial for preventing joint injury and developing shoulder implants. Finite element (FE) models of the shoulder joint can be helpful in describing these forces and the biomechanics of the joint. Currently, there are no validated FE models of the intact shoulder available in the public domain. This study aimed to develop and validate a shoulder FE model, then make the model available to the orthopaedic research community. Publicly available medical images of the Visible Human Project male subject's right shoulder were used to generate the model geometry. Material properties from the literature were applied to the different tissues. The model simulated abduction in the scapular plane. Simulated glenohumeral (GH) contact force was compared to *in vivo* data from the literature, then further compared to other *in vitro* experimental studies. Output variable results were within one standard deviation of the mean *in vivo* experimental values of the GH contact force in 0°, 10°, 20°, 30°, and 45° of abduction. Furthermore, a comparison among different analysis precision in the Abaqus/Explicit platform was made. The complete shoulder model is available for download at github.com/OSEL-DAM/ShoulderFiniteElementModel.

Keywords—Open access, Finite Element Analysis (FEA), Computational model, Glenohumeral contact force, Shoulder.

INTRODUCTION

The shoulder is one of the most complicated joints in the human body, encompassing several different articulations, including the glenohumeral (GH) joint, acromioclavicular joint (AC), sternoclavicular joint (SC), and scapulothoracic joint (ST).[12] Studying the biomechanics of the shoulder under different loading conditions is crucial toward understanding the contact forces, loads, and stresses acting on the soft and hard tissues within the joint. However, measuring internal stresses and contact forces *in vivo* is difficult. Finite element (FE) models with the required level of fidelity capable of replicating the intact shoulder anatomy may serve as alternatives. A reliable FE model should satisfy three conditions: (a) an accurate representation of the joint geometry and material properties, (b) appropriate application of interactions, loads, and boundary conditions, and finally (c) a rigorous validation for the indicated context of use.[26,52]

The collection of FE studies available in the literature provide valuable insights on shoulder biomechanics, however, like all computational models there are limitations to their application. Early FE studies included two-dimensional models of the glenohumeral

Address correspondence to Andrew P. Baumann, Center for Devices and Radiological Health, Office of Science and Engineering Laboratories, Division of Applied Mechanics, U.S. Food and Drug Administration, 10903 New Hampshire Avenue, Building 62 Room 2210, Silver Spring, MD 20993, USA. Electronic mail: Andrew.Baumann@fda.hhs.gov

joint.[30,34,43] Recent studies used three-dimensional models to evaluate the biomechanics of the joint more completely. Several models included just a few major components[13,20,36,49] and limited material behavior to linear elasticity. Over time, more components were added to the FE models such as more detailed representation of the geometries, hyper-elastic properties for the humeral cartilage, glenoid cartilage, and labrum, and anisotropic non-linear elastic properties for the ligaments and tendons.[24] Few studies included the labrum in combination with other major deformable joint components.[22,27] Mostly, the labrum was excluded in shoulder FE studies.[15,16,50] When the labrum was included, there were often other simplifications such as modeling the humeral cartilage as a rigid body.[14,16] Bones were almost always modeled as rigid bodies.[15,16,22,25,27] In addition to the limitations referenced above, none of the models were available in an open-source platform. Making models freely available through an open-source platform can often facilitate more rapid advancement through collaboration and data-sharing.

With the advances in technology over the years, a higher accuracy in representing the joint geometry, material properties, loads, and boundary conditions has become more achievable. However, not all studies report the details of a robust simulation validation.[11,30,36,49] For example, some models were validated to other numerical studies, potentially amplifying any deviations from the actual anatomy.[34,43] Therefore, a freely available validated FE glenohumeral joint would aid the biomechanics community in future development of shoulder research. To the authors' knowledge, there are no validated shoulder FE models available in the public domain. Other open-source FE models do exist, but they often have specific applications that make them inadequate for accurate glenohumeral joint biomechanics representation. For example, the open-source full-body VIVA OpenHBM Finite Element 50th Percentile Female Occupant Model[31] was developed for whiplash studies. Although powerful, its limitations as a shoulder model include simplifications of the joint soft tissues (e.g., no labrum), assigning the bones rigid body properties, using stiffer material properties for the soft tissues, an absence of muscle activations, and not validating for specific shoulder loads and stresses.

The primary aim of this study was to develop an open-source FE model of the shoulder joint with the fidelity required to better capture the physiological behavior of the joint and validate it for a specific context of use against experimental data from the literature, expanding the utility beyond that of previous models. The context of use is limited to the quantification of GH contact force during humeral abduction. The purpose of developing an open-source shoulder FE model is to allow other researchers to perform additional verification and validation studies and leverage the model in their research. It will also allow others to modify, expand, and build upon the model by optimizing details or investigating components such as shoulder implants.

The secondary aim of this study was to investigate the effects of analysis and packager precision on computational cost and accuracy of the results in Abaqus/Explicit. This will aid researchers to make an informed decision on which type of analysis precision will be more suited for their specific problem with the tradeoff being between speed and accuracy.

MATERIALS AND METHODS

Model Construction

Model geometry was generated from computed tomography (CT) scans of the Visible Human Project (US National Library of Medicine)[2] male subject right shoulder. Mimics v15.0 (Materialise, Leuven, Belgium) was used to segment the 3D geometry of the various tissues. Surface geometries were created for the humerus, scapula, clavicle, labrum, and acromioclavicular ligament. These structures were imported to MeshMixer (Autodesk, San Rafael, CA, USA) and MeshLab[6] for further smoothing. The model mesh was generated with 3-matic 7.0 (Materialise, Leuven, Belgium). Quadratic tetrahedral 3D elements were used for all parts. Meshed geometries were then imported into Abaqus/Explicit 6.14–5 (SIMULIA, Providence, RI, USA) for model assembly (Fig. 1) and mesh convergence. The element type assigned in Abaqus was C3D10M. Anatomical position of the model components was evaluated to direct final positioning of the model in Abaqus and correct misalignment associated with the cadaver specimen. Position modifications included adjusting the acromiohumeral distance (i.e., the superior/inferior position of the humeral head relative to acromion),[9] retroversion of the humerus,[28] and shape of the humeral cartilage to account for the humeral head bare area reported in anatomic studies.[10] An orthopaedic surgeon directed final placement of all tissues/components.

Humeral and glenoid cartilages were modeled as thin layers covering their respective underlying bones with thicknesses consistent with the literature.[19,35] Material properties were applied to all components with values taken from the literature (Table 1). Bones were modeled as linear elastic and soft tissues were modeled as neo-Hookean hyper-elastic.[5,21,38,39] Portions of the bones away from the areas of interest

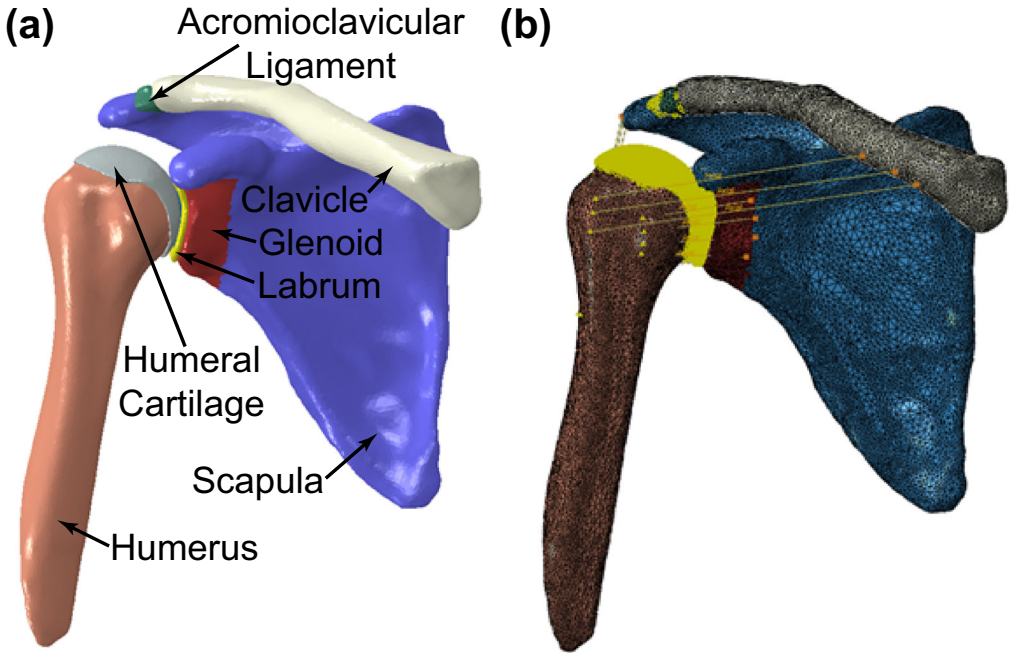

FIGURE 1. (a) Model of the intact shoulder in Abaqus highlighting the different bones (humerus, clavicle, scapula, and glenoid) and soft tissue (humeral and glenoid cartilages, AC ligament, and labrum) components. (b) Meshed view of the model highlighting interactions and muscle 2D connectors.

TABLE 1. Material properties for the FE model.

Anatomy	Material type	Parameters
Scapula	Linear elastic	E = 16 GPa, ν = 0.3[8]
Humerus (Cortical Bone)	Linear elastic	E = 12 GPa, ν = 0.3[7]
Humerus (Cancellous Bone)	Linear elastic	E = 250 MPa, ν = 0.3[7]
Clavicle	Linear elastic	E = 17 GPa, ν = 0.3[17]
Glenoid	Linear elastic	E = 1.4 GPa, ν = 0.3[49]
Acromioclavicular (AC) Ligament	Hyper-elastic	C10 = 1.125 MPa, D1 = 0.19[39]
Glenoid Cartilage	Hyper-elastic	C10 = 1.79 MPa, D1 = 0.12[5,21]
Humeral Cartilage	Hyper-elastic	C10 = 1.79 MPa, D1 = 0.12[5,21]
Labrum	Hyper-elastic	C10 = 12.5 MPa, D1 = 0.017[38]

(humeral shaft, scapula body, and medial clavicle) were modeled as rigid bodies for computational efficiency. Explicit surface to surface hard contact with the "kinematic contact method" and "finite sliding" formulation was used for interactions between the humeral and glenoid cartilages and between the humeral cartilage and the labrum. The penalty friction formulation with a coefficient of friction of 0.01 was applied to these surface-to-surface contacts.[33] The humeral cartilage, glenoid cartilage, and labrum were fixed in all degrees of freedom to their respective underlying bone tissue using tie constraints. Muscle–tendon unit attachments for the rotator cuff (supraspinatus, infraspinatus, subscapularis, and teres minor), middeltoid, and clavicular head of the pectoralis major were modeled as several 2D connector elements. The insertional footprint of the rotator cuff was derived from literature,[10] and the coordinate system of the joint for applying loads and boundary conditions was defined based on the International Society of Biomechanics (ISB) recommendations on the definition of joint coordinate systems.[47]

Mesh Convergence Study

Meshes of decreasing element size were created for all 3D geometries in 3-matic. Average element size was reduced for each iteration such that the number of elements in the model was approximately doubled from one iteration to the next. Element size was not a

global parameter and was controlled within components to account for localized concentrations. Output parameters of maximum contact force, contact area, maximum contact pressure, and maximum von-Mises stress were extracted and compared from one mesh size iteration to the next. These output parameters were evaluated at the GH joint contact, including humeral cartilage, glenoid cartilage, and labrum. The iterations continued until less than 5% deviation in the output variable was achieved. Mass scaling was used to reduce solution time. Strain energies were monitored throughout the simulation to ensure the artificial energy remained acceptably low.

Model Validation

The model was validated for the context of use of predicting GH contact force during a single simulated humeral abduction scenario. Simulated GH contact force during humeral abduction was compared to values reported in the literature. The simulation included two steps: (1) while the scapula was fixed in all degrees of freedom, an initial compression was applied to the humerus to bring the humeral and glenoid cartilage in contact, (2) 100° of glenohumeral abduction in the scapular plane was applied to the humerus through displacement/rotation control boundary conditions applied to the GH joint center which was also the reference point of the humerus rigid body. The scapula was fixed in all degrees of freedom and the scapular elevation was not considered. Muscle forces published by Yanagawa *et al.*[48] were applied to the connector elements representing muscle–tendon unit lines of action. Total force applied by muscles was 206.74 N. All simulations were performed in Abaqus using double precision. The model was considered validated for the context of use if simulation predictions of GH contact force were within one standard deviation (SD) from the mean reported *in vivo* experimental values.[4] Validation beyond this context of use was not considered.

Analysis Precision Effect

After model validation, the simulation was repeated on the model using three different precision settings. The first had the analysis and the packager in single precision mode. The second had the analysis in double precision with the packager in single precision. The third had both the analysis and the packager in double precision. GH contact forces and CPU times were compared across these three precision settings.

RESULTS

Mesh Convergence Results

Mesh convergence was achieved with less than 5% deviation after five iterations. Therefore, the mesh from iteration four was chosen as the converged mesh and used in subsequent simulations (Fig. 2 and Table 2).

Model Validation Results

Outputs of the GH contact force during abduction were extracted from the model and ranged from 84 to 586 N during 0° to 75° of abduction, respectively. This output was compared with *in vivo* data from studies by Bergmann *et al.* (Table 3 and Fig. 3).[3,4] Results of our study were within 1 SD of the mean experimental *in vivo* values throughout the arc of 0° up to but not including 75° of abduction. The peak contact force from our study was 586.14 N. This is within the range of the peak contact force (624.93 ± 149.19 N) reported from the *in vivo* experiments of the six subjects analyzed by Bergmann *et al.*[4]

Analysis Precision Effect Results

The abduction simulation was repeated three times using different analysis and packager precision settings in Abaqus/Explicit. Results for GH contact forces were plotted and compared between the three simulations (Fig. 4). Overall, the three force responses were very close (root mean square error, RMSE, less than 2.2 N), and in the case of this model, any of the precisions would lead to satisfactory results for GH contact forces. There were subtle differences at peak load and higher abduction angles. At these extremes, double precision for both the analysis and packager may lead to a smoother force response. Nevertheless, RMSE values for both single/single and double/single precision relative to double/double were very small (2.18 N and 1.45 N, respectively) for this specific output under these loads and boundary conditions. Execution times were determined for the model run on 84 CPUs on the Ohio Super Computer[1] for (1) analysis and packager set to single, (2) analysis set to double and packager set to single, and (3) analysis and packager set to double were approximately 15, 22, and 23 h, respectively. The model was also run on 8 CPUs with single precision to make sure that users who do not have access to high computational power would be able to utilize the model; the simulation completed in 17.5 h. The model was developed in Abaqus v6.14. Testing using Abaqus 2020 produced similar outcomes.

DISCUSSION

An open-source FE model of the intact shoulder has been developed and validated against *in vivo* experimental data for the context of use of predicting GH contact forces during humeral abduction.

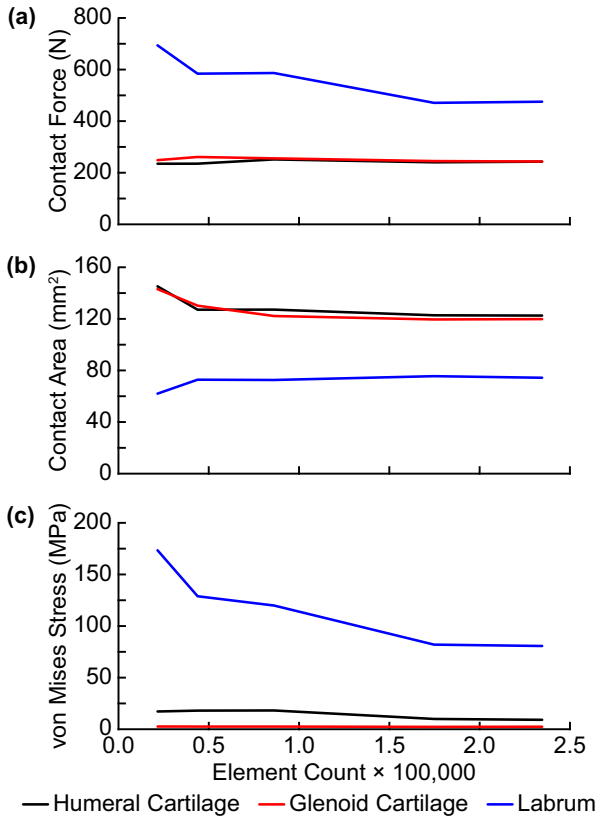

FIGURE 2. Mesh convergence plots depicting the change of (a) Contact Force, (b) Contact Area, and (c) von Mises Stress in the humeral cartilage, glenoid cartilage, and labrum as the number of elements was increased in the soft tissue geometries.

Although other human body FE models are available in the public domain, such as the VHP-Female full-body human CAD model,[40] they lack specificity to the shoulder that prevents them from being readily functional for FE analysis of the shoulder joint. This specificity includes surface-to-surface interactions between contacting components, mesh convergence, and validation of the shoulder biomechanics relative to *in vivo* measurements. In this study, these additional requirements for a practical model have been addressed. This enables the research community to utilize the model for their own purposes such as adding more details or components for shoulder implants, researching kinematics from motion analysis experiments, and evaluating internal forces, moments, and muscle loads from musculoskeletal analyses. All these research questions can be tackled without having to recreate the cumbersome initial steps of image segmentation, model construction, and mesh convergence.

The effect of analysis precision in Abaqus/Explicit was also evaluated for the current model. The smoothest contact force response was achieved while using double precision for both analysis and packager. If accuracy is of greatest concern as well as smooth output variable response, double precision for both analysis and packager is recommended. However, if computational cost is a concern during future simulations, the model could be run in single precision with significantly reduced runtime and produce results that deviate less than 2.1% from full double precision mode. Simulation of a porcine liver deformation under a surgical tool pressure using single and double precision in Abaqus/Explicit showed similar levels of accuracy in both cases with 40% shorter time for the single precision case.[23] Future work will need to explore the effect of precision in more complicated and less stable simulations.

In its present form, the model is stable when simulating abduction. This is likely due to several factors. The first is the highly controlled loading and boundary

TABLE 2. Maximum and minimum element edge lengths and element count for the final converged mesh for each component of the model.

Component	Maximum element edge length (mm)	Minimum Element edge length (mm)	Average max edge length (mm)	Average min edge length (mm)	Element count
Scapula	7.19	0.43	3.76	1.75	55,349
Humerus	7.35	0.40	4.08	2.08	39,827
Clavicle	6.00	0.58	3.83	1.77	16,511
AC Ligament	3.31	1.07	2.24	1.44	2,111
Glenoid Cartilage	1.08	0.09	0.74	0.47	36,551
Humeral Cartilage	1.40	0.13	1.03	0.65	73,736
Labrum	0.73	0.14	0.52	0.34	124,307

TABLE 3. Comparison of glenohumeral contact force at 0°, 10°, 20°, 30°, 45°, and 75° abduction between the current study and different subjects from the *in vivo* experiments done by Bergmann *et al.*[3,4]

	Glenohumeral contact force at each abduction angle (N)					
Study	0°	10°	20°	30°	45°	75°
Subject from Ref. [3]	98.06	222.40	347.52	452.15	574.04	N/A
Subject S8R from Ref. [4]	257.03	244.17	225.45	219.75	309.28	569.73
Subject S2R from Ref. [4]	30.34	35.69	46.58	65.14	223.09	490.79
Subject S3L from Ref. [4]	123.48	136.01	122.41	146.75	236.23	357.92
Mean *in vivo*	127.23	159.57	185.49	220.95	335.66	472.81
SD *in vivo*	95.04	94.88	130.55	166.57	163.38	107.04
Current study	84.25	89.67	136.91	212.3	362.12	586.00

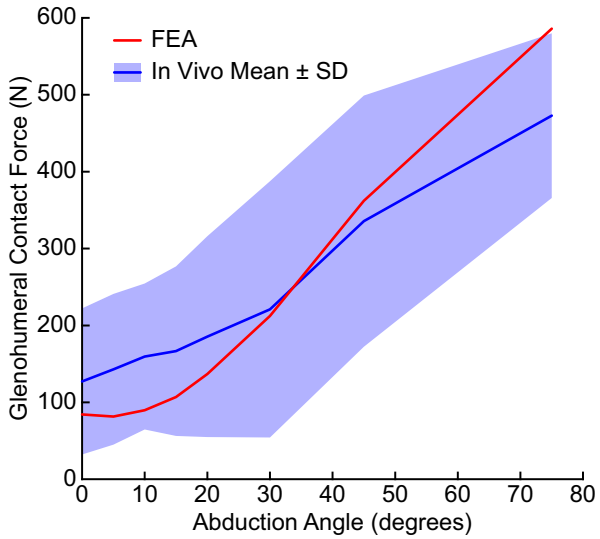

FIGURE 3. Comparison of glenohumeral contact force for the current study during 75° of abduction with the mean experimental values from Bergmann *et al.*[3,4] Blue line: mean *in vivo* (*In vivo* Mean); Blue shaded area: *in vivo* standard deviation (SD); Red line: our finite element outputs (FEA).

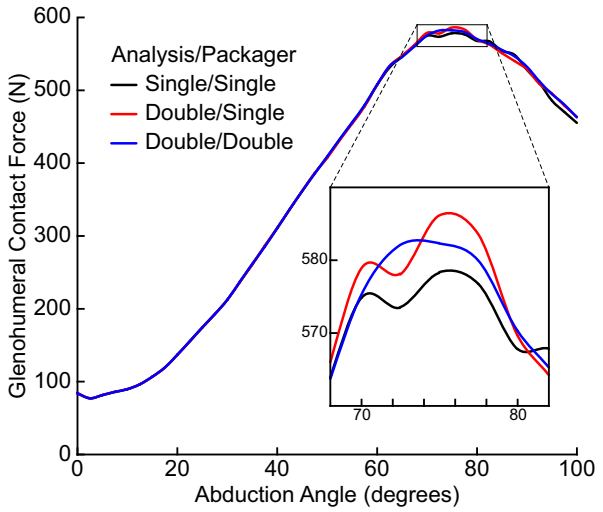

FIGURE 4. Glenohumeral contact force as a function of abduction angle using single and double precision analysis/packager combinations in Abaqus/Explicit.

conditions. These prevent anomalous or unpredictable motions. Other simulations may be less bounded and exhibit greater instability. Such instances may call for additional validation exercises. The second is the robust mesh convergence that ensures results are not mesh dependent. The refined mesh also allows high stress, strain, and/or contact pressure gradients to be examined (though these outputs have not been validated). Future simulations that incorporate orthopaedic devices such as shoulder implants would require additional mesh convergence exercises. Mesh independence will have to be demonstrated if geometries in the model change significantly.

The Bergmann *et al.* studies are a common source for *in vivo* data for computational studies, including some of the references used in this study.[18,37,51] Our outputs were in good agreement with the literature, remaining within 1 SD of the average *in vivo* experimental values during abduction in the scapular plane from 0° up to but not including 75° (Fig. 3). Although there was good agreement with the averaged data, the model does not mimic any single subject's *in vivo* data for the magnitude of the load over the trajectory, where 3 of the 4 subjects exhibited little change in GH contact force over the range of 0° to 30° of abduction.

Although not chosen as the reference for validation, another commonly referenced study is from Poppen *et al.*[32] who reported GH contact forces for three cadaveric male specimens under 150° abduction. Their reported values were 0.38 ± 0.03BW, 0.66 ± 0.16BW, and 0.88 ± 0.13BW for 30°, 60°, and 90° of abduction, respectively. In comparison, our model produced values of 0.24BW, 0.57BW, and 0.60BW for 30°, 60°, and 90° of abduction, respectively. Because the Bergmann study presents *in vivo* data, it was selected as the benchmark to validate our model.

Using the output of a computational model to validate another can introduce and compound error, therefore, we did not use any *in silico* data to validate our model. However, it is still relevant to understand how this model's output compares to other *in silico* studies. The GH contact force at 0°, 10°, 20°, 30°, 45°, and 75° of abduction were extracted from the model and compared with other computational studies in the literature (Table 4). Results from the current model were in agreement with the average of the reported data in the literature for 10°, 20°, 30°, 45°, and 75° abduction. The exception was at 0°, where our output exceeded the average of the reported *in silico* data by more than 1 SD. All of the *in silico* studies used for comparison reported a lower GH contact force than our study and only one produced a GH contact force that was within 1 SD of the average *in vivo* experimental data for 0° (Table 3). While our model remained within 1 SD of the *in vivo* average between 0° to 45° abduction, none of the *in silico* studies used for comparison were within 1 SD from 0° to 45° abduction (Fig. 5). Values were not reported for 0° and 10° of abduction in the study by Sins *et al.* [37] and for 45° of abduction in the study by Zheng *et al.*[51] Angles reported by Sins *et al.* also showed close agreement with *in vivo* data. However, this was a musculoskeletal study for simulating total shoulder arthroplasties and not a finite element model of the intact shoulder. Additionally, their boundary conditions allowed more rotational freedom than the current model.

The intent of creating an open-source FE model is for others to freely build or expand on this work, however there are limitations that the user will need to take into consideration. First, the model was validated for the limited context of use of predicting GH contact forces under simulated humeral abduction. Other contexts of use were not evaluated, and the model cannot be considered validated for other scenarios. Additionally, the standard deviation of the *in vivo* data was quite large, creating a wide validation range and weakening the validity of the model. Also, the validation efforts showed promising outcomes in agreement with other models with different geometries, but only one geometry from one gender was used in this study; therefore, caution should be taken while generalizing the results to other subjects. Future studies should focus on developing open-source models from different population percentiles for both genders, thereby representing a range of subjects.

The element type also presented a limitation. The version of Abaqus used in this work does not support the C3D10 element type for explicit simulations, therefore, C3D10M was used. This type of element has limitations, such as lower stable time increment, greater computational expense, and less accuracy relative to C3D10. However, choosing smaller size elements, as in the case of this study, can mitigate the effect of accuracy reduction.

Another limitation of the model was the 2D representation of the muscles; therefore, no muscle stress information can be produced. However, stresses on the muscles were not the scope of this study, and muscles were modeled as a means of proper application of muscle loads from previous literature or outputs of musculoskeletal modeling. In addition, other studies that modeled muscles as three-dimensional structures[50] have only accounted for the passive behavior of those muscles.

In addition, the glenohumeral abduction motion in this study was applied in a controlled manner by limiting the other degrees of freedom and fixing the scapula in place, not accounting for the scapular rhythm. Arm elevation has two components of glenohumeral and scapulothoracic motion.[29] These two motions happen synchronously, and the resultant motion is called scapulohumeral rhythm. By increasing the arm elevation, the scapula rotates upward, externally, and posteriorly. Not including these motions in the model affects muscle activities. However, muscle activity was not the outcome of this study, and muscle forces were inputs into the model. As future researchers build on the current model, they may modify the degrees of freedom of the model based on their own specific simulation requirements and add the scapulohumeral rhythm to investigate the performance of muscles.

To make an objective comparison between the computational model and *in vivo* data, abduction of the humerus as a basic motion was chosen for simulation. This is a limitation of our study, as only one loading scenario was investigated. This is driven in part because there is currently only one known study in the literature that reports *in vivo* data in the scapular plane and the data is limited to 4 to 6 subjects, depending on the loading scenario.[4] Future efforts should focus on collecting additional comparator data and ensuring the model remains valid when simulating additional motions.[44–46]

Cartilage surfaces and muscle–tendon-unit attachments were estimated from the literature and created under an orthopaedic surgeon's supervision. However, this limitation could be resolved by using MR images instead of CT scans to obtain the exact geometries and attachment locations. Lastly, the joint capsule elements and most of the ligaments were not included in this model. This approach was used for simplification and computational efficiency and has been used by other researchers as well.[5,27] Future studies may add 3D or 2D ligamentous and capsule structures to the current model.

TABLE 4. Glenohumeral contact force for the current study and other *in silico* computational studies from the literature

	Glenohumeral contact force at each abduction angle (N)					
Study	0°	10°	20°	30°	45°	75°
van der Helm *et al.*[42]	16	60	117	164	227	344
Terrier *et al.* [41]	36	145	265	362	488	602
Favre *et al.*[18]	29	100	221	457	544	403
Sins *et al.*[37]	N/A	N/A	157	235	329	546
Zheng *et al.*[51]	8.18	91.45	146.1	408	N/A	N/A
Mean	22.30	99.11	181.22	325.20	396.92	473.82
SD	12.54	35.09	60.30	122.17	145.37	120.11
Current study	84.25	89.67	136.91	212.3	362.12	586.00

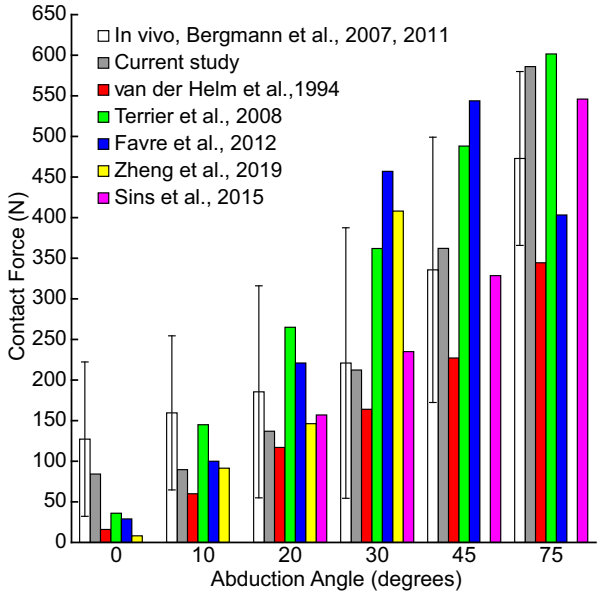

FIGURE 5. Comparison of contact force for the computational studies reported in Table 4 and *in vivo* experiments by Bergmann *et al.*[3,4], at 0°, 10°, 20°, 30°, 45°, and 75° of abduction. The average of *in vivo* data is from the data in Table 3 and the error bars show 1 SD.

In conclusion, this study successfully developed an open-source finite element shoulder model. Prediction of GH contact forces during humeral abduction was validated to within 1 SD of the average experimental *in vivo* data available in the literature. This model was intentionally created using only public data to enable future users to freely leverage, manipulate, and build on information given for any stage of the model development. Such a model is just a start to a library of open-source shoulder FE models to be expanded to cover more population and cases. The complete shoulder model is available for download at github.com/OSEL-DAM/ShoulderFiniteElementModel.

ACKNOWLEDGMENTS

This project was funded by the FDA Critical Path Initiative. Graduate student supplemental funding was provided through a grant from the NSF Non-Academic Research Internships for Graduate Students (INTERN) program for experiential learning through non-academic research internships facilitated through the Center for Disruptive Musculoskeletal Innovations (CDMI). Disclaimer: The mention of commercial products, their sources, or their use in connection with material reported herein is not to be construed as an actual or implied endorsement of such products by US DHHS.

CONFLICT OF INTEREST

The authors have no conflicts of interest.

REFERENCES

[2]Ackerman, M. J. The visible human project. *Proc. IEEE.* 52(Pt 2):1030–1032, 1998.

[3]Bergmann, G., F. Graichen, A. Bender, M. Kaab, A. Rohlmann, and P. Westerhoff. *In vivo* glenohumeral contact forces–measurements in the first patient 7 months postoperatively. *J. Biomech.* 40:2139–2149, 2007.

[4]Bergmann, G., F. Graichen, A. Bender, A. Rohlmann, A. Halder, A. Beier, and P. Westerhoff. *In vivo* gleno-humeral joint loads during forward flexion and abduction. *J. Biomech.* 44:1543–1552, 2011.

[5]Buchler, P., N. A. Ramaniraka, L. R. Rakotomanana, J. P. Iannotti, and A. Farron. A finite element model of the shoulder: application to the comparison of normal and osteoarthritic joints. *Clinical Biomechanics.* 17:630–639, 2002.

[6]Cignoni, P., M. Callieri, M. Corsini, M. Dellepiane, F. Ganovelli and G. Ranzuglia. Meshlab: an open-source mesh processing tool. In: *Eurographics Italian chapter conference* Salerno, Italy, 2008, p. 129–136.

[7]Clavert, P., M. Zerah, J. Krier, P. Mille, J. F. Kempf, and J. L. Kahn. Finite element analysis of the strain distribution in the humeral head tubercles during abduction: comparison of young and osteoporotic bone. *Surg Radiol Anat*. 28:581–587, 2006.

[8]Couteau, B., P. Mansat, E. Estivalezes, R. Darmana, M. Mansat, and J. Egan. Finite element analysis of the mechanical behavior of a scapula implanted with a glenoid prosthesis. *Cli.n Biomech. (Bristol, Avon)*. 16:566–575, 2001.

[9]Culham, E., and M. Peat. Functional anatomy of the shoulder complex. *J. Orthop. Sports Phys. Ther*. 18:342–350, 1993.

[10]Curtis, A. S., K. M. Burbank, J. J. Tierney, A. D. Scheller, and A. R. Curran. The insertional footprint of the rotator cuff: an anatomic study. *Arthroscopy*. 22:609, 2006.

[11]Debski, R. E., J. A. Weiss, W. J. Newman, S. M. Moore, and P. J. McMahon. Stress and strain in the anterior band of the inferior glenohumeral ligament during a simulated clinical examination. *J. Shoulder Elbow. Surg*. 14:24S-31S, 2005.

[12]Delgado, P., S. Alekhya, A. Majidirad, N. A. Hakansson, J. Desai, and Y. Yihun. Shoulder kinematics assessment towards exoskeleton development. *Appl. Sci*. 10:6336, 2020.

[13]Drury, N. J., B. J. Ellis, J. A. Weiss, P. J. McMahon, and R. E. Debski. Finding consistent strain distributions in the glenohumeral capsule between two subjects: implications for development of physical examinations. *J. Biomech*. 44:607–613, 2011.

[14]Drury, N. J., B. J. Ellis, J. A. Weiss, P. J. McMahon, and R. E. Debski. The impact of glenoid labrum thickness and modulus on labrum and glenohumeral capsule function. *J. Biomech. Eng*.132:121003, 2010.

[15]Ellis, B. J., R. E. Debski, S. M. Moore, P. J. McMahon, and J. A. Weiss. Methodology and sensitivity studies for finite element modeling of the inferior glenohumeral ligament complex. *J. Biomech*. 40:603–612, 2007.

[16]Ellis, B. J., N. J. Drury, S. M. Moore, P. J. McMahon, J. A. Weiss, and R. E. Debski. Finite element modelling of the glenohumeral capsule can help assess the tested region during a clinical exam. *Comput. Methods Biomech. Biomed. Eng*. 13:413–418, 2010.

[17]Favre, P., P. Kloen, D. L. Helfet, and C. M. Werner. Superior versus anteroinferior plating of the clavicle: a finite element study. *J Orthop Trauma*. 25:661–665, 2011.

[18]Favre, P., M. Senteler, J. Hipp, S. Scherrer, C. Gerber, and J. G. Snedeker. An integrated model of active glenohumeral stability. *J. Biomech*. 45:2248–2255, 2012.

[19]Fox, J. A., B. J. Cole, A. A. Romeo, A. K. Meininger, J. M. Williams, R. E. Glenn Jr., J. Bicos, J. K. Hayden, and C. B. Dorow. Articular cartilage thickness of the humeral head: an anatomic study. *Orthopedics*. 31:216, 2008.

[20]Gatti, C. J., J. D. Maratt, M. L. Palmer, R. E. Hughes, and J. E. Carpenter. Development and validation of a finite element model of the superior glenoid labrum. *Ann. Biomed. Eng*. 38:3766–3776, 2010.

[21]Huang, C.-Y., A. Stankiewicz, G. A. Ateshian, and V. C. Mow. Anisotropy, inhomogeneity, and tension–compression nonlinearity of human glenohumeral cartilage in finite deformation. *J. Biomech*. 38:799–809, 2005.

[22]Hwang, E., J. E. Carpenter, R. E. Hughes, and M. L. Palmer. Effects of biceps tension and superior humeral head translation on the glenoid labrum. *J. Orthop. Res*. 32:1424–1429, 2014.

[23]Idkaidek, A., and I. Jasiuk. Toward high-speed 3D nonlinear soft tissue deformation simulations using Abaqus software. *J. Robot. Surgery*. 9:299–310, 2015.

[24]Iwamoto, M., K. Miki, and K. H. Yang. Development of a finite element model of the human shoulder to investigate the mechanical responses and injuries in side impact. *JSME Int. J. Ser. C*. 44:1072–1081, 2001.

[25]Jang, S. W., Y. S. Yoo, H. Y. Lee, Y. S. Kim, P. K. Srivastava, and A. V. Nair. Stress distribution in superior labral complex and rotator cuff during *in vivo* shoulder motion: a finite element analysis. *Arthroscopy*. 31:2073–2081, 2015.

[26]Kiapour, A., A. M. Kiapour, V. Kaul, C. E. Quatman, S. C. Wordeman, T. E. Hewett, C. K. Demetropoulos, and V. K. Goel. Finite element model of the knee for investigation of injury mechanisms: development and validation. *J. Biomech. Eng*.136:011002, 2014.

[27]Klemt, C., D. Nolte, G. Grigoriadis, E. Di Federico, P. Reilly, and A. M. J. Bull. The contribution of the glenoid labrum to glenohumeral stability under physiological joint loading using finite element analysis. *Comput. Methods Biomech. Biomed. Eng*. 20:1613–1622, 2017.

[28]Kronberg, M., L. A. Brostrom, and V. Soderlund. Retroversion of the humeral head in the normal shoulder and its relationship to the normal range of motion. *Clin. Orthop. Relat. Res*. 15:113–117, 1990.

[29]Ludewig, P. M., T. M. Cook, and D. A. Nawoczenski. Three-dimensional scapular orientation and muscle activity at selected positions of humeral elevation. *J. Orthop. Sports Phys. Therapy*. 24:57–65, 1996.

[30]Luo, Z.-P., H.-C. Hsu, J. J. Grabowski, B. F. Morrey, and K.-N. An. Mechanical environment associated with rotator cuff tears. *J. Shoulder Elbow Surgery*. 7:616–620, 1998.

[1]Ohio Supercomputer Center. 1987.

[31]Östh J., M. Mendoza-Vazquez, A. Linder, M. Y. Svensson and K. Brolin. The VIVA OpenHBM finite element 50th percentile female occupant model: whole body model development and kinematic validation. In: *IRCOBI Conference*2017, p. 173–181.

[32]Poppen, N., and P. Walker. Forces at the glenohumeral joint in abduction. *Clin. Orthop. Related Res*. 25:165–170, 1978.

[33]Sakai, N., Y. Hagihara, T. Furusawa, N. Hosoda, Y. Sawae, and T. Murakami. Analysis of biphasic lubrication of articular cartilage loaded by cylindrical indenter. *Tribol. Int*. 46:225–236, 2012.

[34]Sano, H., I. Wakabayashi, and E. Itoi. Stress distribution in the supraspinatus tendon with partial-thickness tears: an analysis using two-dimensional finite element model. *J. Shoulder Elbow Surgery*. 15:100–105, 2006.

[35]Schleich, C., B. Bittersohl, G. Antoch, R. Krauspe, C. Zilkens, and J. Kircher. Thickness distribution of glenohumeral joint cartilage: a normal value study on asymptomatic volunteers using 3-tesla magnetic resonance tomography. *Cartilage*. 8:105–111, 2017.

[36]Seki, N., E. Itoi, Y. Shibuya, I. Wakabayashi, H. Sano, R. Sashi, H. Minagawa, N. Yamamoto, H. Abe, K. Kikuchi, K. Okada, and Y. Shimada. Mechanical environment of the supraspinatus tendon: three-dimensional finite element model analysis. *J. Orthop. Sci*. 13:348–353, 2008.

[37]Sins, L., P. Tétreault, N. Hagemeister, and N. Nuño. Adaptation of the AnyBody^{TM} musculoskeletal shoulder model to the nonconforming total shoulder arthroplasty context. *J. Biomech. Eng*. 137:15, 2015.

[38]Smith, C. D., S. D. Masouros, A. M. Hill, A. L. Wallace, A. A. Amis, and A. M. J. Bull. The Compressive Behavior of the Human Glenoid Labrum May Explain the Common Patterns of SLAP Lesions. *Arthrosc. J. Arthrosc. Relat. Surgery*. 25:504–509, 2009.

[39]Sung-Woo, K., J. M. Cavanaugh, J. P. Leach, and S. W. Rouhana. Mechanical properties of the shoulder ligaments under dynamic loading. *Stapp Car Crash J*. 48:125, 2004.

[40]Tankaria H., X. J. Jackson, R. Borwankar, G. N. Srichandhru, A. Le Tran, J. Yanamadala, G. M. Noetscher, A. Nazarian, S. Louie and S. N. Makarov. VHP-female full-body human CAD model for cross-platform FEM simulations—Recent development and validations. In: *2016 38th Annual International Conference of the IEEE Engineering in Medicine and Biology Society (EMBC)*IEEE, 2016, p. 2232–2235.

[41]Terrier, A., A. Vogel, M. Capezzali, and A. Farron. An algorithm to allow humerus translation in the indeterminate problem of shoulder abduction. *Med. Eng. Phys*. 30:710–716, 2008.

[42]Van der Helm, F. C. Analysis of the kinematic and dynamic behavior of the shoulder mechanism. *J. Biomech*. 27:527–550, 1994.

[43]Wakabayashi, I., E. Itoi, H. Sano, Y. Shibuya, R. Sashi, H. Minagawa, and M. Kobayashi. Mechanical environment of the supraspinatus tendon: a two-dimensional finite element model analysis. *J. Shoulder Elbow. Surg*. 12:612–617, 2003.

[44]Westerhoff, P., F. Graichen, A. Bender, A. Halder, A. Beier, A. Rohlmann, and G. Bergmann. *In vivo* measurement of shoulder joint loads during activities of daily living. *J. Biomech*. 42:1840–1849, 2009.

[45]Westerhoff, P., F. Graichen, A. Bender, A. Halder, A. Beier, A. Rohlmann, and G. Bergmann. *In vivo* measurement of shoulder joint loads during walking with crutches. *Clin. Biomech*. 27:711–718, 2012.

[46]Westerhoff, P., F. Graichen, A. Bender, A. Halder, A. Beier, A. Rohlmann, and G. Bergmann. Measurement of shoulder joint loads during wheelchair propulsion measured *in vivo*. *Clin. Biomech*. 26:982–989, 2011.

[47]Wu, G., F. C. Van der Helm, H. D. Veeger, M. Makhsous, P. Van Roy, C. Anglin, J. Nagels, A. R. Karduna, K. McQuade, and X. Wang. ISB recommendation on definitions of joint coordinate systems of various joints for the reporting of human joint motion—Part II: shoulder, elbow, wrist and hand. *J. Biomech*. 38:981–992, 2005.

[48]Yanagawa, T., C. J. Goodwin, K. B. Shelburne, J. E. Giphart, M. R. Torry, and M. G. Pandy. Contributions of the individual muscles of the shoulder to glenohumeral joint stability during abduction. *J. Biomech. Eng*.130:021024, 2008.

[49]Yeh, M.-L., D. Lintner, and Z.-P. Luo. Stress distribution in the superior labrum during throwing motion. *Am. J. Sports Med*. 33:395–401, 2005.

[50]Zheng, M. X., Z. H. Qian, Z. M. Zou, C. Peach, M. Akrami, and L. Ren. Subject-specific finite element modelling of the human shoulder complex part 1: model construction and quasi-static abduction simulation. *J. Bionic Eng*. 17:1224–1238, 2020.

[51]Zheng, M. X., Z. H. Qian, Z. M. Zou, C. Peach, and L. Ren. Subject-specific finite element modeling of the human shoulder complex part 2: quantitative evaluation of the effect of rotator cuff tear propagation on glenohumeral joint stability. *IEEE Access*. 7:34068–34077, 2019.

[52]Zheng, M. X., Z. M. Zou, P. J. D. Bartolo, C. Peach, and L. Ren. Finite element models of the human shoulder complex: a review of their clinical implications and modelling techniques. *Int. J. Numerical Methods Biomed. Eng*.33:e02777, 2017.